Article (refereed) - postprint

Adams, Jessica L.; Tipping, Edward; Feuchtmayr, Heidrun; Carter, Heather T.; Keenan, Patrick. 2018. **The contribution of algae to freshwater dissolved organic matter: implications for UV spectroscopic analysis**.

This is an Accepted Manuscript of an article published by Taylor & Francis Group in *Inland Waters* on 15/01/2018, available online: https://doi.org/10.1080/20442041.2017.1415032

Second revision submitted to Inland Waters September 2017

The contribution of algae to freshwater dissolved organic matter: implications for UV spectroscopic analysis

Jessica L. Adams*, Edward Tipping, Heidrun Feuchtmayr, Heather T. Carter, Patrick Keenan

Centre for Ecology & Hydrology, Lancaster Environment Centre, Lancaster, LA1 4AP, UK

*Corresponding author: Jessica L. Adams jesams@ceh.ac.uk

ABSTRACT

Dissolved organic matter (DOM) is an important constituent of freshwater. It participates in a number of key ecological and biogeochemical processes, and can be problematic during water treatment. Thus, the demand for rapid and reliable monitoring is growing and spectroscopic methods are potentially useful. A model with 3 components, 2 absorbing in the ultraviolet (UV) range and present at variable concentrations, and a third that does not absorb light and is present at a low constant concentration, was previously found to give good predictions of dissolved organic carbon concentration; [DOC]. However, the model underestimated [DOC] in shallow, eutrophic lakes in the Yangtze Basin, China, raising the possibility that DOM derived from algae might be poorly estimated. This is supported by new data reported here for eutrophic British lakes. We estimated the extinction coefficients, in the UV range, of algae-derived DOM, from published data on algal cultures, and from new data from outdoor mesocosm experiments in which high concentrations of DOC were generated under conditions comparable to those in eutrophic freshwaters. The results demonstrate the weak UV absorbance of DOM from algae compared to DOM from terrestrial sources. A modified model, in which the third component represents algae-derived DOM present at variable concentrations, allowed contributions of such DOM to be estimated by combining the spectroscopic data with [DOC] measured by laboratory combustion. Estimated concentrations of algae-derived DOC in 77 surface freshwater samples ranged from zero to 8.6 mg L^{-1}, and the fraction of algae-derived DOM ranged from zero to 100%.

Key words: absorption spectroscopy, algal products, dissolved organic carbon, eutrophication, modelling

Introduction

Dissolved organic matter (DOM) is ubiquitous in surface, soil and ground waters, and chiefly comprises partially decomposed plant and animal material (Thurman 1985). It provides a source of energy for microbes, controls absorption of light and photochemical activity, participates in nutrient cycling, buffers pH, sorbs metals and other organic pollutants, and interacts with nanoparticles (Tipping 2002, Aiken et al. 2011, Tipping et al. 2016). Reactions of DOM with chlorine during drinking water treatment produce by-products including trihalomethanes and haloacetic acids, which are a risk to human health (Nguyen et al. 2005). The need to monitor the quality and quantity of DOM has increased considerably in recent years, partly because of the widespread observed increases in concentrations and fluxes of dissolved organic carbon (DOC) in surface waters (Monteith et al. 2007), which have implications for ecology and the costs of water treatment. The DOM produced by algae is important in lake carbon cycling and storage (Heathcote et al. 2012) and is especially problematic in water treatment (Nguyen et al. 2005, Henderson et al. 2008, Ly et al. 2017).

Dissolved organic matter is routinely quantified by the dissolved organic carbon concentration [DOC], for example by infra-red detection of carbon dioxide (CO_2) after combustion. Significant correlations between optical absorbance and [DOC] mean that approximate quantification can be achieved from UV-visible absorption spectroscopy at a single wavelength (e.g., Grieve 1984, Moore 1987).

However, the spectroscopic properties of DOM vary temporally and spatially, a fact that is exploited for example in the well-known use of specific ultra-violet absorbance (SUVA) as an indicator of DOM quality (Chin et al. 1994, Weishaar et al. 2003). Such variability means that the single wavelength approach cannot generally provide an accurate measure of [DOC].

Therefore, Tipping et al. (2009) developed a 2-component model employing UV absorbance data at 2 wavelengths, and showed that it could provide precise estimates of [DOC] in a variety of surface water samples.

The 2-component model adopted the linear sum of the concentrations of component A (DOC_A) and component B (DOC_B) representing strongly and weakly UV-absorbing material, respectively. Further development of this modelling approach by Carter et al. (2012) introduced a third component, 'component C', which represents non UV-absorbing DOC, assumed to be present at the same concentration in all samples. The total [DOC] is then the linear sum of [DOC_A], [DOC_B] and [DOC_C]. Testing this 3-component model with data for 1700 river and lake samples (but few eutrophic waters) resulted in good, unbiased predictions of [DOC] ($r^2 = 0.98$) with fixed spectroscopic characteristics of the end members A and B, combined with a small constant concentration of component C at 0.8 mg L^{-1}. Because [DOC_C] was fixed, the model still only required absorbance data at 2 wavelengths. The dual wavelength approach was therefore suggested as a means to estimate [DOC] accurately, rapidly, and inexpensively, without the need for lengthier laboratory processing and measurement and for *in situ* field monitoring.

However, for eutrophic shallow lakes of the Yangtze basin (Zhang et al. 2005), the model underestimated [DOC] by an average factor of 2.1 (Carter et al. 2012). The average extinction coefficient (absorbance/[DOC]) of 6.5 L g^{-1} cm^{-1} at 280 nm in these samples suggested the presence of material that absorbs UV light more weakly than either component A or B. Further, Zhang et al. (2005) found a positive relationship between DOM fluorescence and the extent of eutrophication of the different Yangtze basin lakes, which indicated possible influences from algal production. Therefore, it appears that the 3-component, dual wavelength model may be effective only when the DOM under consideration is predominantly terrestrial in origin. Consequently, further investigation of the optical

properties of algae-derived DOM, and how they affect the performance of the model, is necessary.

UV spectroscopic data for DOM derived from different algal species grown in laboratory cultures have been reported by Nguyen et al. (2005) who worked with axenic (sterilised) cultures, and by Henderson et al. (2007) who worked with non-axenic cultures. Nguyen et al. (2005) reported that the DOM produced comprised labile carbohydrates and proteins with low SUVA values compared to those of terrestrially-sourced DOM. Henderson et al. (2007) also found the DOM to absorb UV light weakly. De Haan and De Boer (1987) concluded, from field observations of [DOC] and UV absorbance of the humic lake Tjeukemeer, that water entering from the neighbouring eutrophic lake Ijsselmeer brought weakly UV-absorbing DOM. Osburn et al. (2011) studied saline waters of the prairie lakes region of the USA, which were rich in DOM of autochthonous (i.e., algal) origin, created by bacterial processing of primary production, and reported optical absorption at 350 nm. Their values were appreciably lower than those commonly observed for waters with comparable [DOC] but with terrestrial sources of DOM (Carter et al. 2012). The results of these different studies are consistent in suggesting that algae-derived DOM absorbs UV light weakly compared to DOM from terrestrial sources.

Although these laboratory and field observations suggest that DOM derived from algae has different absorption characteristics from terrestrially sourced material, they do not permit a general quantitative assignment of spectroscopic parameters. We added to the data from algal cultures reported by Nguyen et al. (2005) and Henderson et al. (2007) by making new measurements on DOM generated by algae growing in outdoor mesocosms, under conditions arguably more realistic than those in the cultures. Then we evaluated these combined data to quantify UV absorption at different wavelengths, by deriving representative extinction coefficients, for algae-derived DOM.

The new absorption parameters were then used to analyse the data for a new freshwater sample set, biased towards eutrophic water bodies, to estimate concentrations of algae-derived DOM and the fraction of total [DOC] that they account for. By this means, we aimed to quantify the contribution of algae-derived DOM to freshwater [DOC], and to UV absorbance, in order to (1) evaluate how the presence of such DOM in water samples would affect estimation of [DOC] by UV spectroscopy, and (2) provide a means to quantify DOM from different sources (the terrestrial system and algae) in rivers and lakes.

Study Site

Surface water samples representative of different states of eutrophication (defined by [Chl-*a*]) and DOM source were collected from catchments in the North of England during the summer and autumn of 2014 and 2015 (Table 1, Tables S1a and S1b). The Shropshire – Cheshire meres are situated in the North-West Midland outwash plains and drain predominantly small agricultural, urban, and parkland catchments (Reynolds 1979, Moss et al. 2005). Fisher et al. (2009) reported a range of 2–68 μg L^{-1} for average chlorophyll *a* concentration, [Chl-*a*], across the Shropshire – Cheshire meres region (Table S1a). Ten of the samples were from small lakes in the Lake District National Park and 4 were from reservoirs in West Yorkshire, all of which drain upland moorland. Ten further sites included small farm ponds in the Fylde area of Lancashire and rivers and small streams draining lowland arable farmland and urban areas in Yorkshire.

Methods

Application of the 3 component model of Carter et al. (2012)

The measure of optical properties used here is the extinction coefficient of the sample (*E*), also known as specific absorbance, which is the ratio of the absorbance at a given wavelength to [DOC] with units L g^{-1} cm^{-1} (Tipping et al. 2009). The basis of the model of Carter et al. (2012) is that the DOM that absorbs UV light can be represented as a mixture of 2 components, A and B, each with a defined UV spectrum. The fraction of component A (f_A) is given by

$$f_A = \frac{E_{B,\lambda 1} - R\, E_{B,\lambda 2}}{R\,(E_{A,\lambda 2} - E_{B,\lambda 2}) + (E_{B,\lambda 1} - E_{A,\lambda 1})} \qquad (1)$$

140 where E_A and E_B are the extinction coefficients of components A and B at 2 given

141 wavelengths ($\lambda 1$ and $\lambda 2$) and R is the measured ratio of absorbance at the same 2

142 wavelengths. The value of f_A can then be substituted into the following equation to obtain the

143 extinction coefficient for the sample being measured

144 $$E_{AB,\lambda} = f_A E_{A,\lambda} + f_B E_{B,\lambda} = f_A E_{A,\lambda} + (1 - f_A) E_{B,\lambda} \quad (2)$$

145 where $E_{AB,\lambda}$ is the extinction coefficient of the sample at either of the 2 chosen wavelengths

146 and f_A and f_B are the fractions of components A and B ($f_A + f_B = 1$).

147 To calculate the total UV-absorbing [DOC], the measured absorbance at either of the

148 wavelengths is divided by $E_{AB,\lambda}$ from equation (2), and the total (absorbing + non-absorbing)

149 [DOC] is obtained by adding a constant [DOC_C] representing a small amount of non-

150 absorbing DOM present at the same concentration (0.8 mg L^{-1}) in all water samples

151 $$[DOC] = \frac{A_\lambda}{E_{AB,\lambda}} + [DOC_C] \quad (3)$$

152 Where the choice of wavelengths for the calculation is flexible, as long as they differ

153 sufficiently (by about 50 nm or more). Carter et al. (2012) reported extinction coefficients for

154 a number of wavelengths in the range 254 – 355 nm, and used various combinations to

155 analyse published data. The model is best-applied to filtered samples (as used in the present

156 work) and is assumed to apply to all freshwaters irrespective of pH or ionic composition.

157 Henceforth, we refer to the 3 component model with fixed [DOC_C] as the Carter model.

158

159 *Mesocosm experiments*

160 The mesocosms are part of the CEH aquatic mesocosm facility (CAMF);

161 http://www.ceh.ac.uk/our-science/research-facility/aquatic-mesocosm-facility, accessed

162 January 2017. The facility contains 32 mesocosms, each of 2 metre diameter and 1 metre

163 depth, simulating shallow lakes. Of the 32 mesocosms used for a multiple stressor

164 experiment, 4 were selected (mesocosms 4, 7, 15 and 20) to obtain a range of Chl-*a*

concentrations. In the stressor experiment, the mesocosms were subjected to different treatments, including heating (4^0C above ambient) and the addition of nutrients free from nitrogen or phosphorus. Mesocosms 4 and 20 were both unheated, with an average ambient water temperature of 14.6^0C over the sampling period, and with intermittent nutrient addition. Mesocosm 7 was heated with intermittent nutrient addition, and mesocosm 15 was heated without intermittent nutrient addition. Sampling took place on 7 occasions between February and August 2015. The dominant algal classes for each of the four mesocosms were Chlorophyceae and Cyanophyceae, with a bloom of *Euglena* in mesocosm 7 in the early summer. For our analyses, a 500 mL sample was collected from the four mesocosms in pre-rinsed vessels.

We assumed that the DOM produced in the mesocosms during the observation period resulted from the fixation of atmospheric CO_2 by algae and its subsequent release in DOM. Although some allochthonous sources could influence the mesocosm DOM, these can be disregarded for the following reasons: (1) The simulation experiments commenced in 2013, when sediment from a natural lake was added to the mesocosms, and therefore there has been enough time for DOM in the water column to come to equilibrium with the sediment, (2) An increase in pH could provide a mechanism for releasing DOM from sediment (Tipping 2002), but during our observation period there were no systematic changes in pH, and thus it is reasonable to assume that net DOM release did not occur, and (3) Addition of allochthonous DOM to the mesocosms may have occurred through rainfall, but rainwater [DOC] is typically low, around 0.6 mg L^{-1} for parts of the UK (Wilkinson et al. 1997) and < 2 mg L^{-1} globally (Willey et al. 2000); quite insufficient to generate the large observed increases in [DOC].

Laboratory analyses

189 All samples were processed within 3 days of collection. Owing to the fact that the mesocosms
190 were primarily used for a separate study, there were minor methodological differences
191 between the analyses of the field and mesocosm samples. The determination of algal [Chl-*a*]
192 in field samples followed the method of Maberly et al. (2002). A known volume of the
193 sample was filtered through a Whatman GF/F (0.7 µm) filter paper, which was then
194 immediately submerged in 10 mL of industrial methylated spirit (IMS, 96% ethanol, 4%
195 methanol) and left overnight, in the dark at 4ºC. The mesocosm samples were analysed
196 similarly for [Chl-*a*], but using a Whatman GF/C (1.2 µm) filter paper, which was submerged
197 in 96 % ethanol. The 2 different extraction solvents (IMS and 96% ethanol) are known to be
198 equally efficient (Jespersen and Christoffersen 1987). Following centrifugation at 4500 rpm,
199 optical absorbance readings at 665 and 750 nm were used to calculate [Chl-*a*], following
200 Marker et al. (1980). The mesocosm samples collected on 12 August 2015, were analysed for
201 [Chl-*a*] *in situ* using an AlgaeTorch (bbe Moldaenke, Germany), which had been calibrated
202 against [Chl-*a*] data obtained by ethanol extraction for all 32 mesocosms over the preceding
203 8-month period, yielding a regression with R^2=0.67 (n=442, p<0.0001). Field samples were
204 analysed for pH and conductivity using a glass electrode with a Radiometer instrument and a
205 Jenway 4510 probe respectively, each instrument being calibrated for each set of samples.
206 For the mesocosm experiment, pH and conductivity were measured *in situ*, using a Hydrolab
207 DS5X multiparameter data sonde (OTT Hydromet), except that for samples collected on 12
208 August 2015 and 26 September 2015, pH and conductivity were measured using an EXO2
209 multiparameter data sonde (Exowater). Both multiparameter sondes were calibrated in the
210 laboratory before sampling the mesocosms.
211 All samples for absorbance spectroscopy and the determination of [DOC] were
212 analysed by the same procedure. A 125 mL sub-sample was filtered using a Whatman GF/F
213 (0.7 µm) filter. A 3 mL filtered sample was measured for absorbance in the UV-Vis range

(200 nm – 900 nm) using an Agilent 8453 diode array spectrophotometer with a 1 cm path length quartz cuvette. Prior to each sample batch, measurements were made on a blank using Milli-Q water, and used to correct the spectra of the samples. A 10 mg L^{-1} solution of naphthoic acid was used as a quality control. Absorbance values at 270 nm, 350 nm and 700 nm were selected for [DOC] calculation with the model of Carter et al. (2012). Values of A_{270} and A_{350} for the calculations were obtained by subtracting A_{700} (near zero) from the raw values to correct for instrument drift; it also corrects for suspended matter in unfiltered samples, although these were not used in the present work. The remaining sample was acidified with 3 M hydrochloric acid and purged with zero grade air for 4 minutes to remove any inorganic carbon. The sample was then combusted at 905°C with cobalt chromium and cerium oxide catalysts, which converts all the remaining carbon to CO_2. The CO_2 was measured for [DOC] through infra-red detection using a Skalar Formacs CA16 analyser.

Mathematical apportionment of DOM forms

The procedure to apportion 3 DOM forms (A, B and C, or A, B and C2) from measured values of UV absorbance and [DOC] was as follows. Note that here we assume that component C (no absorbance) or C2 (absorbance characteristics from Table 2) is present at a variable concentration, and so the description differs from the Carter model which has fixed [DOC_C]. For simplicity, the following description is only in terms of A, B and C. The total absorbance at a given wavelength is given by the linear sum of the absorbances of the 3 components

$$A_\lambda = A_{\lambda A} + A_{\lambda B} + A_{\lambda C}, \qquad (4)$$

and can be expressed in terms of the total DOC concentration, the fraction of each component in the mixture (f_A, f_B, f_C), and their extinction coefficients ($E_{\lambda A}$, $E_{\lambda B}$, $E_{\lambda C}$)

$$A_\lambda = [DOC]\ \{f_A E_{\lambda A} + f_B E_{\lambda B} + f_{C2} E_{\lambda C}\}. \qquad (5)$$

If A_λ and [DOC] are known from measurement, then since f_A, f_B and f_{C2} must total unity, equation (5) has 2 unknowns (e.g., f_A and f_B), and to calculate them it is necessary to have measured values of A_λ for 2 different, sufficiently separated, wavelengths (λ_1 and λ_2). Since the measurements cannot be error-free, the values of f_A and f_B cannot be calculated by solution of simultaneous equations, and instead were estimated by minimisation of squared residuals in observed and calculated $A_{\lambda 1}$ and $A_{\lambda 2}$. Calculated values ($A_{\lambda 1,calc}$ and $A_{\lambda 2,calc}$) were obtained from equation (5) for trial values of f_A and f_B, and f_C by difference ($1 - f_A - f_B$). The residuals are

$$r_1 = A_{\lambda 1,calc} - A_{\lambda 1,meas}, \quad (6)$$

$$r_2 = A_{\lambda 2,calc} - A_{\lambda 2,meas}, \quad (7)$$

where $A_{\lambda 1,meas}$ and $A_{\lambda 2,meas}$ are the measured absorbances at the 2 wavelengths. The sum of the squared residuals ($r_1^2 + r_2^2$) was minimised by iterative improvement of the trial values of f_A and f_B, to give the best fit of the data. Values of [DOC_A], [DOC_B] and [DOC_C] were obtained from the products of [DOC] with the derived f_A, f_B and f_C respectively.

Statistics and minimisation

Calculations of standard deviations, t-tests, and regression analyses were carried out using Microsoft Excel. The Solver function in Microsoft Excel was used to perform minimisations in the apportionment calculations.

Results

Estimating extinction coefficients for DOM derived from freshwater algae

The 4 selected mesocosms represent enclosed systems where allochthonous inputs are negligible. They therefore simulate conditions where the dominant DOM component is derived from algae, but may be modified by subsequent microbial processing. Measured and modelled [DOC], absorbance data, and [DOC] estimated with the Carter model, are shown in Fig. 1 (see also Table S1c). Absorbance at 270 nm and 350 nm increased slightly through time. The modelled [DOC] also increased slightly, but at a considerably lower rate than the measured [DOC], which rose from 8.2 mg L^{-1} to 63.4 mg L^{-1} in mesocosm 4. The same pattern was also seen in the mesocosms with lower [DOC] such as mesocosm 15, where [DOC] increased from 4.5 mg L^{-1} to 14.1 mg L^{-1}. Extinction coefficients derived from the absorbance and [DOC] results of Fig. 1 decline with [DOC] for both wavelengths (Fig. 2). There was a significant positive relationship ($p < 0.001$) between measured [DOC] and [Chl-*a*] for the mesocosm samples (Table S2). The average pH for the mesocosms was 9.7 and there was no significant relationship observed between measured [DOC] and pH.

The extinction coefficients of the additional DOM produced were estimated by considering the changes in [DOC] and optical absorbance in the mesocosms during the sampling period. First, the increase in [DOC] was calculated for each of the mesocosms by finding the differences between the first data point and each of the last 4. Then, the same was done for the absorbance values at 270 nm and 350 nm, and also for 254 nm, 280 nm and 355 nm to permit comparison with results from other studies. Extinction coefficients were calculated as the averages of the ratios of the absorbance and [DOC] increases during algal growth. Similar results were obtained for the different mesocosms, yielding reasonably well-defined extinction coefficients, which are considerably lower than those estimated by Carter et al. (2012) for terrestrially-derived freshwater DOM (Table 2). We also calculated

extinction coefficients at 254 nm of DOM produced in laboratory cultures from the results of Nguyen et al. (2005) and Henderson et al. (2008). The results of these 2 studies showed only minor differences in the E_{254} values of DOM from different algal species.

The average E_{254} for DOM produced in the mesocosms does not differ significantly (t-test, $p>0.05$) from the value for DOM in the non-axenic cultures (Henderson et al. 2008). Although it is significantly (t-test, $p<0.05$) greater than the value for DOM in the axenic cultures (Nguyen et al 2005), the difference is modest.

Therefore, the results suggest that the UV absorption properties of DOM derived from freshwater algae can reasonably be represented by a single set of extinction coefficients; there is no evidence that different algal species, or collections of species, produce greatly different types of DOM, at least with respect to their UV spectra. For further modelling analysis (see below), we used the average extinction coefficients derived from the mesocosm data.

Natural water samples

Samples collected from the field sites had a wide range of [DOC], from 1.7 mg L^{-1} in a soft water lake to 63.5 mg L^{-1} in a peat dominated lake. Overall, the Carter model predicted [DOC] reasonably well (Fig. 3), with an average modelled:measured ratio of 0.96. However, model predictions for seven sites were too low (average modelled:measured ratio = 0.70) and these were all situated in the Shropshire-Cheshire meres region, which features eutrophic lakes. In our judgement, the results from these 7 sites cannot be satisfactorily explained by the Carter model. Combining the data from all of the Shropshire - Cheshire meres sites with the Yangtze Basin samples (Zhang et al. 2005) shows that the Carter model fails with eutrophic lakes, especially for samples with relatively low [DOC] (Fig. 4).

Spectroscopic modelling with 3 variable components

The underestimation of [DOC] in samples from eutrophic lakes suggests the presence of DOM that absorbs weakly in comparison to the terrestrially-derived components A and B, and is present at concentrations greater than the fixed value of 0.8 mg L^{-1} for component C assumed in the Carter model. Clearly, DOM derived from algae is a likely explanation for this DOM, and so we analysed the data for the natural water samples by assuming the DOM to comprise variable amounts of components A, B and algae-derived DOM, which we refer to as component C2 and which has the extinction coefficients (Table 2) derived as described above. In this application, the model was not used to estimate [DOC]; instead, we combined the measured [DOC] value with spectroscopic data to estimate the fractions of components A, B and C2 in each sample (see Methods). For the new data reported here, we used wavelengths of 270 nm and 350 nm, while for the Yangtze basin samples (Zhang et al. 2005) the wavelengths were 280 nm and 355 nm (Table 2). Errors in the modelled values of f_A, f_B and f_{C2} were estimated (Table S3) using representative errors in the input values (measured UV absorbance and [DOC]) and errors in the extinction coefficients for algae-derived DOM (Table 2). The errors in f_A, f_B and f_{C2} were modest, the largest (average 0.03) being due to uncertainty in [DOC], the next largest (average 0.009) to extinction coefficient errors, and the smallest (average 0.003) to errors in measured absorbance.

The results indicate that algae-derived DOM is most prevalent in the eutrophic Yangtze basin (YB) lakes with a mean [DOC_{C2}] of 4.9 mg L^{-1}, and all f_{C2} values greater than 0.66 (mean = 0.87; Table 3, Fig. 5, Table S4). Of the UK sites, the Shropshire-Cheshire meres (SCM) have the highest amounts of algae-derived DOM; the mean concentration of 3.6 mg L^{-1} for [DOC_{C2}] was appreciably greater than the Carter model fixed [DOC_C] value of 0.8 mg L^{-1}, and this explains why the Carter model predicts [DOC] poorly in some of the samples. However, it remains the case that in only 4 of the 21 SCM samples did f_{C2} exceed 0.5, indicating that the majority of the DOM was from algae. Therefore in most instances the

catchment was the main supplier of DOM to the SCM lakes. For the remaining UK site categories of Table 1 (LD, PR, YR) the mean values of [DOC_{C2}] were in the range 0 to 1.0 mg L^{-1}, with an overall mean of 0.7 mg L^{-1}. This is very similar to the fixed value of [DOC_C] of 0.8 mg L^{-1} (equation 4), which implies that if these samples contain algae-derived DOM then it is present at sufficiently low concentrations to be accounted for by the fixed component C of the Carter model.

The possible dependence of the derived [DOC_{C2}] values on measured [Chl-*a*] was examined by regression analysis for the samples collected and analysed in the present study (Table S5). There was no relationship when all data were analysed together. However, if data for the 5 site categories of Table 1 were analysed separately, there was a positive relationship in each case, although only for LD (n = 10, $r^2 = 0.46$) and FP (n = 5, $r^2 = 0.73$) were the relationships significant ($p<0.05$). Zhang et al. (2005) did not report [Chl-*a*], and so we compared our estimated [DOC_{C2}] values for the YR sites with total phosphorus concentrations; again there was a positive but not significant ($p>0.05$) relationship.

For comparison, we also performed the apportionment calculations with the non-absorbing component C as the third variable, that is, we found f_A, f_B and f_C, together with [DOC_A], [DOC_B] and [DOC_C]. Note that this is different from the Carter model, where [DOC_C] is a constant. The results did not differ greatly from those obtained with C2 (Table S4) and in linear regression there was a strong correlation between the estimates of [DOC_C] and [DOC_{C2}] ($R^2 = 0.99$, $p < 0.001$, n = 77); on average, the calculated values of [DOC_C] were 80% of those of [DOC_{C2}].

For completeness, we examined whether the assumption of a fixed concentration of DOC_{C2}, instead of DOC_C, affected application of the Carter model to data from 426 UK surface water samples previously used by Carter et al. (2012) to derive model parameters. This was done by re-optimisation of the parameters, assuming the weakly UV absorbing

component C2, rather than the non-absorbing C, to be present at a fixed concentration; in other words we attributed all DOM not accounted for by components A and B to algae-derived DOM. The derived parameters using component C2 were almost the same as the original values; the new fitted extinction coefficients for components A and B differed by less than 0.5% from the original ones, and the fixed concentration of C2 was greater by only 0.06 mg L^{-1} than the original fixed concentration of component C.

Discussion

The mesocosm experiments provided a valuable simulation of a eutrophic shallow lake system, and as explained in Methods it could reasonably be assumed that the DOM produced during the observation period resulted from the fixation of atmospheric CO_2 by algae and its subsequent release in DOM. The assumption is further supported by the highly significant relationship ($P<0.001$) between [DOC] and [Chl-*a*] obtained for the mesocosms (Table S2). In the mesocosms, the relationship is likely strengthened by both the high [Chl-*a*] and the lack of flushing, so that the production of DOM (Fig. 1) follows the change in algal biomass fairly closely. This is less likely in the field sites, where the relationship may be confounded by the time gap between the formation of Chl-*a* by primary production and the subsequent conversion of algal biomass to DOM, together with variations in flushing rates within and between the natural waters. Therefore, although we found that modelled [DOC_{C2}] showed positive relationships with [Chl-*a*] or total [P] (Table S5), the relationships were not strong, and only significant ($P<0.05$) in 2 cases with rather few numbers of samples. Nonetheless, the results overall show that modelled [DOC] generally deviates from the measured value in field waters classified as eutrophic, as judged by their generally relatively high [Chl-*a*] values. This supports the assumption that [DOC] not explained by the Carter model is associated with algae.

The extinction coefficient at 254 nm for DOM derived from algae in the mesocosm experiments (Table 2) is similar in magnitude to the averages of the values for a range of algal species that can be calculated from data reported by Nguyen et al. (2005) and Henderson et al. (2008). We therefore can assume that the UV absorption properties of the mesocosm material are generally representative of algae-derived DOM. The similarity holds for both axenic (Nguyen et al. 2005) and non-axenic (Henderson et al. 2008; our mesocosms) conditions, implying that although bacterial processing of the DOM may affect its

392 composition (Rochelle-Newall et al. 2004) this does not significantly alter its UV spectrum.
393 The UV absorption characteristics of DOM derived from freshwater algae can be compared
394 to those of open ocean DOM, which is largely algal-derived (Biddanda and Benner 1997, Jiao
395 et al. 2010). We estimated UV extinction coefficients for marine DOM from the Mid-Atlantic
396 Bight region by combining absorbance data (Helms et al. 2008) with a measured [DOC] of
397 0.9 mg L^{-1} (Guo et al. 1995). We obtained values at 270 nm and 350 nm of 6.4 L g cm^{-1} and
398 1.0 L g cm^{-1} respectively, which are similar to the freshwater values of Table 2. The much
399 lower extinction coefficients of DOM derived from algae, compared to those for terrestrially-
400 sourced DOM (components A and B; Table 2) must reflect the paucity of conjugated or
401 aromatic moieties in algal biomass; in particular algae lack the lignin phenols that account for
402 the spectra of terrestrial DOM (Del Vecchio and Blough 2004).
403 We focused here on eutrophic waters in which algae-derived DOM was expected to
404 be present. In this context it was justified to replace component C in the Carter model by
405 component C2, which has the UV absorption characteristics of algae-derived material; this is
406 equivalent to assuming that all the DOM not attributable to components A and B was algal in
407 origin. Then the contributions of algae-derived DOM in the different waters could be
408 estimated by optimising the values of f_A, f_B and f_{C2} (Table 3, Fig. 5). This approach provides
409 the best estimates of [DOC_A], [DOC_B] and [DOC_{C2}] for the present samples, and
410 demonstrates that C2 can be the dominant component, particularly in the Yangtze basin lakes
411 (Zhang et al. 2005), total [DOC] values of which were poorly predicted by the Carter model.
412 More extreme examples of freshwaters in which autochthonous sources dominate the DOM
413 are the 27 saline, generally eutrophic, prairie lakes of the U.S.A. Great Plains, studied by
414 Osburn et al. (2011). These had [DOC] in the range 13 to 330 mg L^{-1} (median 28 mg L^{-1}), and
415 the mean whole-sample extinction coefficient at 350 nm was 1.5 (SD 1.1) L $gDOC^{-1}$ cm^{-1}, in
416 fair agreement with our value for algae-derived DOM (Table 2).

Another circumstance in which significant amounts of weakly-absorbing DOM occur was reported by Pereira et al. (2014), who found that headwater streams of tropical rainforests in Guyana contained between 4.1% and 89% optically "invisible" DOM following rainfall events, the likely sources of the material being fresh leaf litter and/or topsoil. The "invisible" DOM was taken to be the difference between DOM measured by combustion and that estimated with the Carter model. It may be that the material identified by Pereira et al. (2014) was not truly invisible, that is, completely lacking in chromophores; rather it may have been weakly-absorbing, as for algae-derived DOM. It is unlikely that the DOM from these terrestrial sources is the same as the algae-derived DOM of Table 2, and so it would have different extinction coefficients. However, because the algae-derived and tropical headwater DOM both have low UV extinction coefficients, then should they occur together there would be little prospect of distinguishing them, especially against a "background" of A and B. For the same reason, when we assumed algae-derived DOM to be the same as component C (i.e., non-UV-absorbing), the estimates of [DOC_C] were quite similar to (on average 80% of) the estimates of [DOC_{C2}] (Table S4).

Implications for UV spectroscopic analysis

Apportionment of DOM forms using measured [DOC]: The approach used in the present work allowed the contribution of algae-derived DOM to the total to be estimated, using combustion-measured [DOC] as an input to the calculation, and with the extinction coefficients estimated from the mesocosm results. This type of analysis could be useful in biogeochemical and ecosystem studies of eutrophic freshwaters. It could also benefit the characterisation of DOM in water undergoing treatment for supply, bearing in mind the difficulty of treating algae-derived DOM (see Introduction). If the absorption characteristics of the non-A, non-B material could be determined or assumed, the analysis method could be

used in other circumstances. For example, it might be applied to the tropical headwaters studied by Pereira et al. (2014); as noted above, Pereira et al. (2014) assumed it to be non-absorbing.

Continued use of Carter model: The samples used by Carter et al. (2012) to obtain [DOC] and absorbance data to construct their model were representative only of temperate freshwaters with mainly allochthonous DOM, formed in terrestrial ecosystems and leached into water courses. It remains the case that for such waters the Carter model is likely to be an accurate and rapid means of both estimating total [DOC] and obtaining information about the division of the DOM between components A and B. For such waters, the assumption of a small amount of component C works satisfactorily, and we showed here that even if a fixed concentration of component C2 were substituted for component C the results would hardly differ. Periodic checking against [DOC] measured by combustion would of course be necessary. The Carter model has considerable potential for use in continuous monitoring, although it would not reveal unexpected excursions from ambient conditions.

Derivation of a "universal" model: The outstanding question is whether the present findings can be exploited to make a "universal" model that would permit [DOC] to be estimated in most or many freshwaters. The logical extension of the Carter model would be to replace the fixed invisible component C by a variable component with a defined UV absorbance spectrum, representative of different contributors, including algae-derived DOM and the DOM in tropical headwaters. As discussed above, incorporation of more than one weakly-absorbing component is unlikely to be feasible. To extract concentrations of 3 components would require data for 3 wavelengths at least. As well as fitting the data to 3 components in a mixing model, information might also be obtained from the spectral slope, following Fichot and Benner (2011); these workers showed, for estuarine water samples, a monotonic relationship between specific absorption (equivalent to extinction coefficient) and

467 the spectral slope in the range 275 to 295 nm. The use of derivative spectra may also prove
468 helpful (Causse et al. 2017). To explore the feasibility of a truly generally-applicable model,
469 absorption and [DOC] data from as wide as possible a range of contrasting waters need to be
470 gathered and analysed. Experience with the Carter model suggests that a model of this type
471 would probably be most effective for water samples with moderate proportions of weakly-
472 absorbing DOM; if weakly-absorbing DOM dominates, calculated total [DOC] would likely
473 prove sensitive to spectral variations among its different types.
474

475 *Conclusions*

476 We have defined, for the first time to our knowledge, generally-applicable average extinction
477 coefficients for algae-derived DOM. The values are based on data from outdoor mesocosm
478 experiments in which high concentrations of algae-derived DOM were generated, supported
479 by literature data from axenic and non-axenic culture experiments with freshwater algae.
480 Combining the extinction coefficients of algae-derived DOM with extinction coefficients for
481 terrestrially-sourced material, and with measured [DOC], permits the apportionment of DOM
482 among the three components. The results show that the algae-derived DOM can account for
483 nearly all the DOM in some eutrophic lakes. The presence of algal DOM and of other forms
484 of weakly-absorbing DOM in tropical headwaters, mean that a previously developed dual
485 wavelength spectroscopic model, assuming 2 variable UV-absorbing components and a fixed
486 concentration of non-UV-absorbing DOM, cannot be applied to all waters. However, that
487 model remains applicable to temperate waters in which terrestrial sources account for most or
488 all of the DOM. A more widely-applicable spectroscopic model for freshwater DOM will
489 require the use of absorbance data for at least 3 wavelengths.
490

491 **Acknowledgements**

This research was funded by the UK Science and Technology Facilities Council CLASP project (Grant No: ST/K00672X/1). The mesocosm experiment was part of the MARS project, funded under the 7th EU Framework Programme (contract no. 603378). We are grateful to J. Richardson, M. De Ville and other team members of the CEH aquatic mesocosm facility (CAMF) for collecting samples and providing data, P. Tipping for help with field sampling, S.C. Maberly for practical guidance, and D.T Monteith and P. Scholefield for helpful comments on the draft manuscript. We thank C. Williams, an anonymous referee, and the Associate Editor R.L. North for their constructive review comments and suggestions.

References

Aiken GR, Hsu-Kim H, Ryan JN. 2011. Influence of dissolved organic matter on the environmental fate of metals, nanoparticles, and colloids. Environ Sci Technol. 45:3196–3201.

Biddanda B, Benner R. 1997. Carbon, nitrogen and carbohydrate fluxes during the production of particulate and dissolved organic matter by marine phytoplankton. Limnol Oceanogr. 42:506-518.

Carter HT, Tipping E, Koprivnjak J-F, Miller MP, Cookson B, Hamilton-Taylor J. 2012. Freshwater DOM quantity and quality from a two-component model of UV absorbance. Water Res. 46:4532-4542.

Causse J, Thomas O, Jung A-V, Thomas M-F. 2017. Direct DOC and nitrate determination in water using dual pathlength and second derivative UV spectrophotometry. Water Res. 108:312-319.

Chin YP, Aiken GR, O'Loughlin E. 1994. Molecular-weight, polydispersity, and spectroscopic properties of aquatic humic substances. Environ Sci Technol. 28:1853–1858.

De Haan H, De Boer T. 1987. Applicability of light absorbance and fluorescence as measures of concentration and molecular size of dissolved organic carbon in humic Lake Tjeukemeer. Water Res. 21:731-734.

Del Vecchio R, Blough NV. 2004. On the origin of the optical properties of humic substances. Environ Sci Technol. 38:3885-3891.

Fichot CG, Benner R. 2011. A novel method to estimate DOC concentrations from CDOM absorption coefficients in coastal waters. Geophys Res Lett. 38:L03610.

Fisher J, Barker T, James C, Clarke S. 2009. Water quality in chronically nutrient-rich lakes: the example of the Shropshire – Cheshire meres. Freshwat Rev. 2:79-99.

Grieve IC. 1984. Determination of dissolved organic matter in streamwater using visible spectrometry. Earth Surf Process Landf 10:75-78.

Guo L, Santschi PH, Warnken W. 1995. Dynamics of dissolved organic carbon (DOC) in oceanic environments. Limnol Oceanogr. 40:1392-1403.

Heathcote AJ, Downing JA. 2012. Impacts of eutrophication on carbon burial in freshwater lakes in an intensively agricultural landscape. Ecosystems. 15:60–70.

Helms JR, Stubbins A, Ritchie JD, Minor EC. 2008. Absorption spectral slopes and slope ratios as indicators of molecular weight, source and photobleaching of chromophoric dissolved organic matter. Limnol Oceanogr 53:955-969.

Henderson RK, Baker A, Parsons SA, Jefferson B. 2008. Characterisation of algogenic organic matter extracted from cyanobacteria, green algae and diatoms. Water Res. 42:3435-3445.

Jespersen AM, Christoffersen K. 1987. Measurements of chlorophyll – *a* from phytoplankton using ethanol as an extraction solvent. Arch Hydrobiol. 109:445-454.

Jiao N, Herndl GJ, Hansell DA, Benner R, Kattner G, Wilhelm SW, Kirchman DL, Weinbauer MG, Luo T, Chen F, Azam F. 2010. Microbial production of recalcitrant dissolved organic matter: long-term carbon storage in the global ocean. Nature Rev Microbiol. 8:593-599.

Ly QV, Maqbool T, Jin Hur J. 2017. Unique characteristics of algal dissolved organic matter and their association with membrane fouling behavior: a review. Environ Sci Poll Res. 24: 11192–11205.

Maberly SC, King L, Dent MM, Jones RI, Gibson CE. 2002. Nutrient limitation of phytoplankton and periphyton growth in upland lakes. Freshwater Biol. 47:2136-2152.

Marker AFH, Nusch EA, Rai H, Riemann B. 1980. The measurement of photosynthetic pigments in freshwaters and standardization of methods: conclusions and recommendations. Archiv fur hydrobiology beihefte ergebnisse der limnologie 14:97-106.

Monteith DT, Stoddard JL, Evans CD, De Wit HA, Forsius M, Hohasen T, Wilander A, Skjelvale BL, Jeffries DS, Vourenmaa J, Keller B, Kopacek J, Vesely J. 2007. Dissolved organic carbon trends resulting from changes in atmospheric deposition chemistry. Nature 450:537-540.

Moore TR. 1987. An assessment of a simple spectrophotometric method for the determination of dissolved organic carbon in freshwaters. N.Z. J Mar Freshwat Res. 21:585-589.

Moss B, Barker T, Stephen D, Williams AE, Balayla DJ, Beklioglu M, Carvalho L. 2005. Consequences of reduced nutrient loading on a lake system in a lowland catchment: deviations from the norm? Freshwater Biol. 50:1687-1705.

Nguyen M-L, Westerhoff P, Baker L, Hu Q, Esparza-Soto M, Sommerfield M. 2005. Characteristics and reactivity of algae produced dissolved organic carbon. J. Environ. Eng. 131:1574-1582.

Osburn CL, Wigdahl CR, Fritz SC, Saros JE. 2011. Dissolved organic matter composition and photoreactivity in prairie lakes of the U.S. Limnol Oceanogr. 56:2371-2390.

Pereira R, Isabella Bovolo C, Spencer RGM, Hernes PJ, Tipping E, Vieth-Hillerbrand A, Pedentchouk N, Chappell NA, Parkin G, Wagner T. 2014. Mobilization of optically invisible dissolved organic matter in response to rainstorm events in a tropical forest headwater river. Geophys Res Lett. 41:1202-1208.

Reynolds CS. 1979. The limnology of the eutrophic meres of the Shropshire-Cheshire plain. Field studies. 5:93-173

575 Rochelle-Newall E, Delille B, Frankignoulle M, Gattuso J-P, Jacquet S, Riebesell U,
576 Terbruggen A, Zondervan I. 2004. Chromophoric dissolved organic matter in
577 experimental mesocosms maintained under different pCO_2 levels. Mar Ecol Prog Ser.
578 272:25-31.
579 Thurman EM. 1985. Organic geochemistry of natural waters. Dordrecht: Kluwer.
580 Tipping E. 2002. Cation binding by humic substances. Cambridge University Press:
581 Cambridge.
582 Tipping E, Corbishley HT, Koprivnjak J-F, Lapworth DJ, Miller MP, Vincent CD, Hamilton-
583 Taylor J. 2009. Quantification of natural DOM from UV absorption at two
584 wavelengths. Environ Chem. 6:472-476.
585 Tipping E, Boyle JF, Schillereff DN, Spears BM, Phillips G. 2016. Macronutrient processing
586 by temperate lakes: a dynamic model for long-term, large-scale application. Sci Tot
587 Environ. 572:1573–1585.
588 Weishaar JL, Aiken GR, Bergamaschi BR, Fram MS, Fuji R, Mopper K. 2003. Evaluation of
589 specific ultra violet absorbance as an indicator of the chemical composition and
590 reactivity of dissolved organic carbon. Environ Sci Technol. 37:4702-4708
591 Wilkinson J, Reynolds B, Neal C, Hill S, Neal M, Harrow M. 1997. Major, minor and trace
592 element composition of cloudwater and rainwater at Plynlimon. Hydrol. Earth Syst
593 Sc. 1:537-569.
594 Willey JD, Kieber RJ, Eyman MS, Brooks Avery Jr G. 2000. Rainwater dissolved organic
595 carbon: concentrations and global flux. Global Biogeochem Cycles. 14:139-148.
596 Zhang Y, Qin B, Zhang L, Zhu G, Chen W. 2005. Spectral absorption and fluorescence of
597 chromophoric dissolved organic matter in shallow lakes in the middle and lower
598 reaches of the Yangtze River. J Freshwater Ecol. 20:451-459.

Tables

Table 1. Mean values of dissolved organic carbon concentration [DOC], pH, conductivity (cond) and chlorophyll concentration [Chl-*a*] for the field sites. Numbers of samples are denoted by *n*. Modelled refers to application of the Carter model.

Code	Site category	*n*	[DOC] mg L^{-1}		pH	cond µs cm^{-1}	[Chl-*a*] µg L^{-1}
			Measured	modelled			
SCM	Shropshire-Cheshire meres	21	14.1	11.7	8.2	358	39.2
LD	Lake District lakes	10	2.9	2.9	7.6	86	14.1
PR	Pennine reservoirs	4	8.9	10.4	7.2	96	16.7
FP	Fylde farmyard ponds	5	21.7	22.6	8.0	311	91.5
YR	Lowland Yorkshire rivers	15	3.9	4.0	7.9	627	14.7

604 Table 2. Extinction coefficients (E_K L g DOC^{-1} cm^{-1}) for dissolved organic matter (DOM)
605 derived from algae, and parameters from the Carter model (components A and B). Mesocosm
606 values were derived from data in Fig. 3, with 16 measurements at each wavelength. The value
607 for axenic cultures is averaged from 12 values of Nguyen et al. (2005), and that for non-axenic
608 cultures is from 4 values of Henderson et al. (2008). Error terms are 95% confidence margins.
609 All E_K values are significantly greater than zero (P<0.001 for E_{254}, E_{270}, E_{280}; P<0.01 for E_{350},
610 E_{355}).

Source	E_{254}	E_{270}	E_{280}	E_{350}	E_{355}
Mesocosms	5.7 (±1.7)	4.9 (±1.4)	4.4 (±1.3)	1.1 (±0.5)	1.0 (±0.5)
Axenic cultures[1]	3.7 (±0.7)	-	-	-	-
Non-axenic cultures[2]	5.4 (±0.4)	-	-	-	-
Model component A	77.1	69.3	63.9	30.0	27.9
Model component B	21.3	15.4	12.0	0.0	0.0

611 [1] Average of results for *Scenedesmus quadricauda*, *Chaetoceros mulleri*, *Oscillatoria*
612 *Prolifera* (Nguyen et al. 2005).
613 [2] Average of results for *Chlorella vulgaris*, *Microcystis aeruginosa*, *Asterionella formosa*,
614 *Melosira* sp., at stationary phase growth (Henderson et al. 2008).
615
616
617

Table 3. Measured dissolved organic carbon concentration [DOC], calculated fractions of A, B and C2, and calculated [DOC_A], [DOC_B] and [DOC_{C2}], ordered by [DOC_{C2}]. See Table 1 for key to the UK sites; sample details are given in Supplemental material 1. YB = Yangtze basin SCM = Shropshire Cheshire meres, LD = Lake District lakes PR = Pennine reservoirs, FP = Fylde farm ponds, YR = lowland Yorkshire rivers.

Sample ID	$[DOC]_{meas}$ mg L^{-1}	f_A	f_B	f_{C2}	$[DOC_A]$ mg L^{-1}	$[DOC_B]$ mg L^{-1}	$[DOC_{C2}]$ mg L^{-1}
YR3b	2.7	0.31	0.69	0.00	0.8	1.9	0.0
YR3a	2.4	0.65	0.35	0.00	1.6	0.9	0.0
PR2	8.9	0.83	0.17	0.00	7.4	1.5	0.0
PR4	8.9	0.42	0.58	0.00	3.7	5.2	0.0
FP3	28.7	0.33	0.67	0.00	9.6	19.1	0.0
PR3	9.6	0.84	0.16	0.00	8.1	1.5	0.0
PR1	8.3	0.70	0.30	0.00	5.9	2.5	0.0
SCM7a	13.8	1.00	0.00	0.00	13.8	0.0	0.0
FP5	32.4	0.67	0.33	0.00	21.8	10.6	0.0
YR2a	2.8	0.40	0.57	0.02	1.1	1.6	0.1
SCM9a	9.9	0.17	0.81	0.01	1.7	8.1	0.1
LD4	2.2	0.26	0.68	0.07	0.6	1.5	0.1
YR5a	3.5	0.36	0.54	0.10	1.2	1.9	0.3
YR4a	3.7	0.22	0.65	0.13	0.8	2.4	0.5
LD10	2.1	0.24	0.54	0.23	0.5	1.1	0.5
LD9	3.9	0.38	0.44	0.19	1.5	1.7	0.7
YR2b	2.3	0.25	0.42	0.32	0.6	1.0	0.8
LD1	3.6	0.24	0.53	0.22	0.9	1.9	0.8
LD2	1.7	0.32	0.20	0.48	0.5	0.3	0.8
LD7	1.9	0.18	0.40	0.42	0.4	0.8	0.8
LD3	2.9	0.19	0.51	0.31	0.6	1.5	0.9
YR2c	3.7	0.29	0.46	0.26	1.1	1.7	1.0
YR3c	3.7	0.28	0.43	0.29	1.0	1.6	1.0
YR4c	3.7	0.24	0.47	0.28	0.9	1.8	1.1
LD6	2.2	0.33	0.16	0.51	0.7	0.4	1.1
YR4b	3.7	0.25	0.43	0.32	0.9	1.6	1.2
YR5c	3.6	0.31	0.32	0.37	1.1	1.2	1.3
FP1	15.3	0.30	0.60	0.09	4.6	9.2	1.4
SCM6a	10.0	0.19	0.66	0.15	1.9	6.6	1.5
YR1c	6.6	0.26	0.50	0.24	1.7	3.3	1.6
YR1a	5.1	0.57	0.12	0.31	2.9	0.6	1.6
YR5b	4.7	0.23	0.43	0.34	1.1	2.0	1.6
LD8	2.8	0.19	0.22	0.59	0.5	0.6	1.6
SCM13	7.4	0.16	0.58	0.26	1.2	4.3	2.0
FP4	14.5	0.23	0.64	0.14	3.3	9.2	2.0
LD5	5.2	0.28	0.31	0.40	1.5	1.6	2.1

Table 3 (continued)

YB8	2.7	0.03	0.15	0.82	0.1	0.4	2.2
SCM8	20.1	0.22	0.64	0.14	4.4	13.0	2.8
SCM14	7.5	0.18	0.45	0.37	1.3	3.4	2.8
SCM3	7.7	0.13	0.50	0.37	1.0	3.8	2.8
SCM16a	11.3	0.11	0.64	0.25	1.2	7.2	2.9
YR1b	7.3	0.19	0.41	0.40	1.4	3.0	2.9
SCM5	10.7	0.12	0.58	0.31	1.3	6.2	3.3
YB22	4.1	0.03	0.13	0.84	0.1	0.5	3.4
YB2	4.9	0.04	0.21	0.76	0.2	1.0	3.7
YB5	4.1	0.03	0.06	0.91	0.1	0.3	3.7
SCM9b	10.9	0.13	0.54	0.34	14	5.9	3.7
FP2	17.8	0.29	0.50	0.21	5.1	9.0	3.7
SCM15	11.5	0.13	0.53	0.33	1.5	6.2	3.8
YB16	4.4	0.03	0.08	0.89	0.1	0.4	3.9
YB19	4.7	0.00	0.15	0.85	0.0	0.7	4.0
SCM12	16.7	0.13	0.63	0.24	2.1	10.5	4.1
YB7	5.6	0.03	0.21	0.76	0.2	1.2	4.3
YB3	4.3	0.00	0.00	1.00	0.0	0.0	4.3
SCM10	7.4	0.08	0.34	0.58	0.6	2.5	4.3
YB13	6.7	0.06	0.28	0.66	0.4	1.9	4.4
SCM4	8.42	0.07	0.40	0.53	0.6	3.4	4.5
SCM16b	11.5	0.09	0.52	0.39	1.1	5.9	4.5
SCM11	7.8	0.07	0.35	0.58	0.5	2.7	4.5
YB4	4.9	0.00	0.04	0.96	0.0	0.2	4.7
YB9	5.6	0.04	0.10	0.86	0.2	0.6	4.8
YB6	5.5	0.01	0.09	0.90	0.0	0.5	4.9
YB18	5.0	0.00	0.02	0.98	0.0	0.1	4.9
SCM6b	11.3	0.09	0.48	0.43	1.0	5.4	4.9
YB1	6.4	0.01	0.18	0.81	0.1	1.1	5.2
YB14	5.8	0.01	0.09	0.90	0.1	0.5	5.2
SCM1	27.7	0.26	0.56	0.19	7.2	15.4	5.2
SCM7b	15.1	0.12	0.53	0.35	1.8	8.0	5.3
YB15	5.6	0.00	0.00	1.00	0.0	0.0	5.6
YB20	6.5	0.00	0.04	0.96	0.0	0.3	6.2
YB21	7.7	0.00	0.13	0.87	0.0	1.0	6.7
YB17	7.5	0.01	0.08	0.91	0.1	0.6	6.8
YB11	8.4	0.06	0.09	0.85	0.5	0.8	7.1
SCM2	63.5	0.47	0.40	0.13	30.1	25.1	8.3
YB12	10.1	0.09	0.06	0.85	0.9	0.6	8.6

625

626 **Figure captions**

627 **Fig. 1** Monthly time-dependence of DOC concentration [DOC] and absorbance for
628 experimental mesocosms; see Methods for experimental treatments. Measured and modelled
629 [DOC] are shown on the primary (left) axis, represented by hollow and filled squares,
630 respectively. Absorbance values at 270 nm and 350 nm are on the secondary (right) axis,
631 represented by filled and hollow triangles, respectively. Mesocosm 4 = panel A, mesocosm 7
632 = panel B, mesocosm 15 = panel C and mesocosm 20 = panel D.

633 **Fig. 2** Extinction coefficients (*E*) at 270 nm (A) and 350 nm (B) plotted against measured
634 [DOC] for the mesocosms. Samples were collected between February and August 2015.

635 **Fig. 3** Comparison of DOC concentration [DOC] estimated using the Carter model with
636 measured [DOC] for all samples collected in this study. Hollow circles represent the mesocosm
637 samples and triangles the field sites. Filled triangles show 7 Shropshire – Cheshire meres sites
638 that were not satisfactorily explained by the Carter model. The 1:1 line is shown.

639 **Fig. 4** Comparison of DOC concentration [DOC] estimated using the Carter model with
640 measured [DOC] for the Shropshire – Cheshire mere water samples (triangles) and Chinese
641 lakes (Zhang et al. 2005; hollow squares).The filled triangles show the 7 mere sites that were
642 unsatisfactorily predicted by the Carter model. The 1:1 line is shown.

643 **Fig. 5** The fraction of the variable component C2 (f_{C2}) vs the [DOC_{C2}] for UK field sites (Table
644 1) and the Yangtze basin (YB) samples. Category PR (Pennine Reservoirs) values are not
645 plotted because all f_{C2} values were close to zero (Table 3).

646

647

648

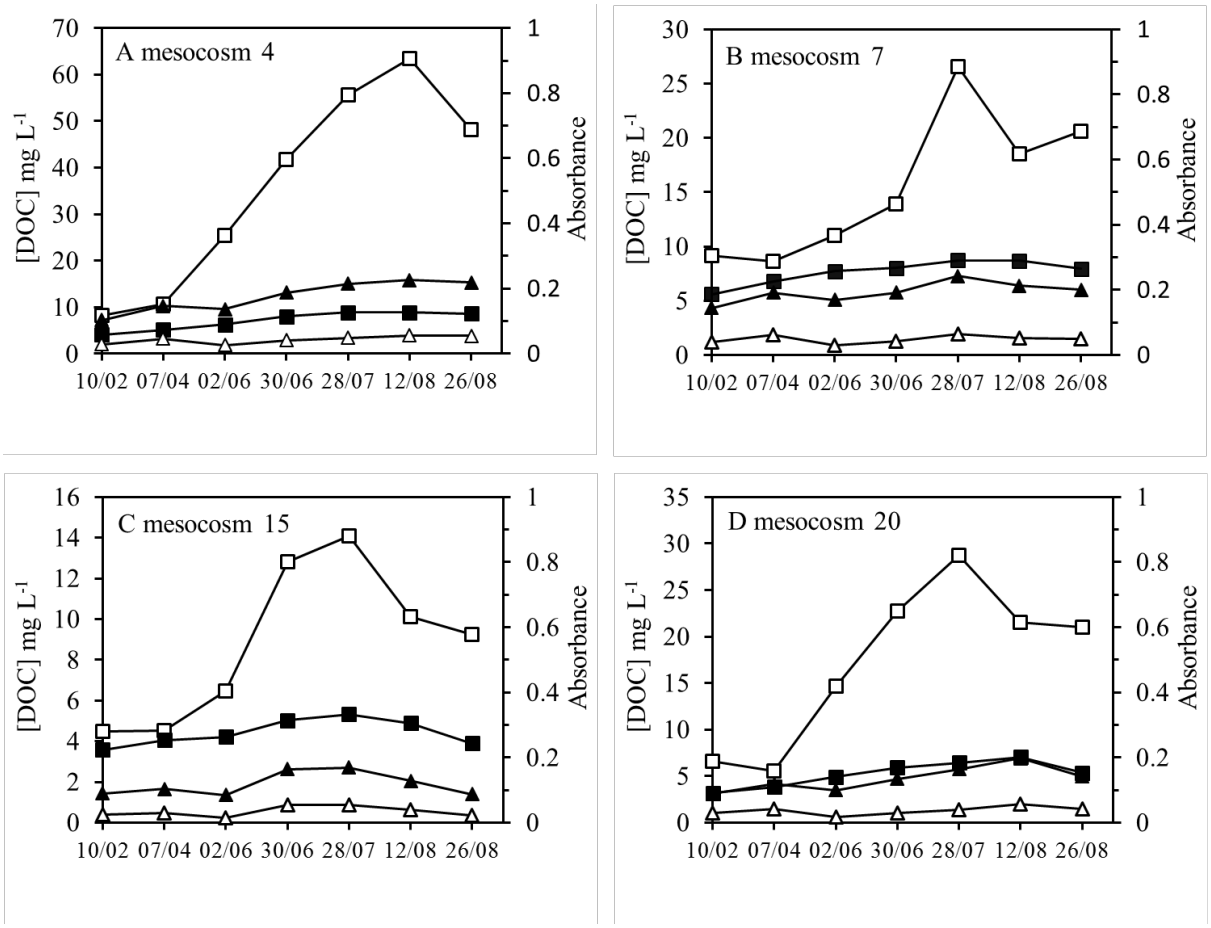
A mesocosm 4
B mesocosm 7
C mesocosm 15
D mesocosm 20
[DOC] mg L-1
Absorbance
10/02 07/04 02/06 30/06 28/07 12/08 26/08

Figure 1

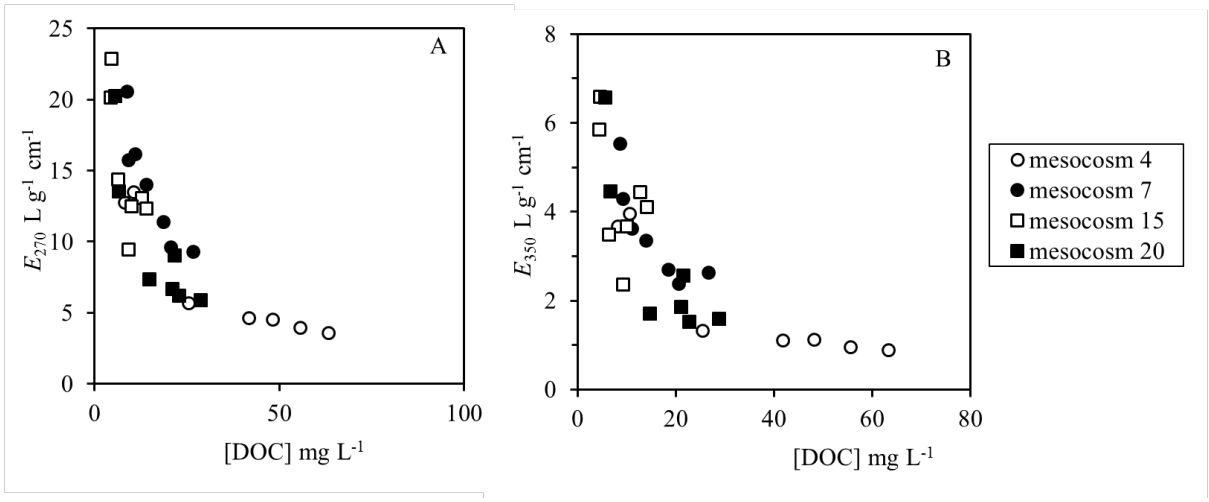
A
B
E_{270} L g^{-1} cm^{-1}
E_{350} L g^{-1} cm^{-1}
[DOC] mg L^{-1}
[DOC] mg L^{-1}
mesocosm 4
mesocosm 7
mesocosm 15
mesocosm 20

Figure 2

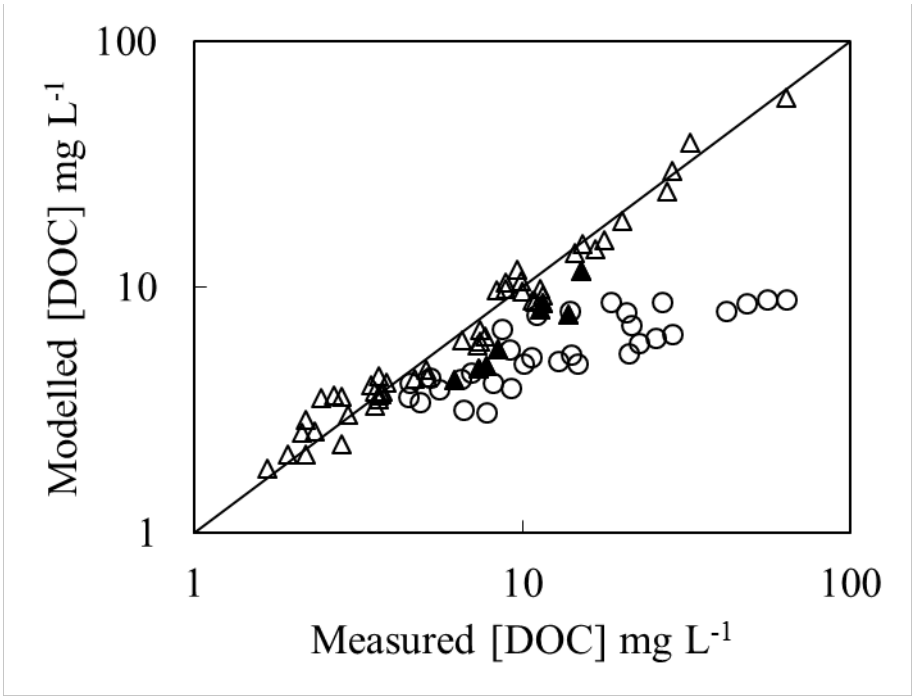

Figure 3

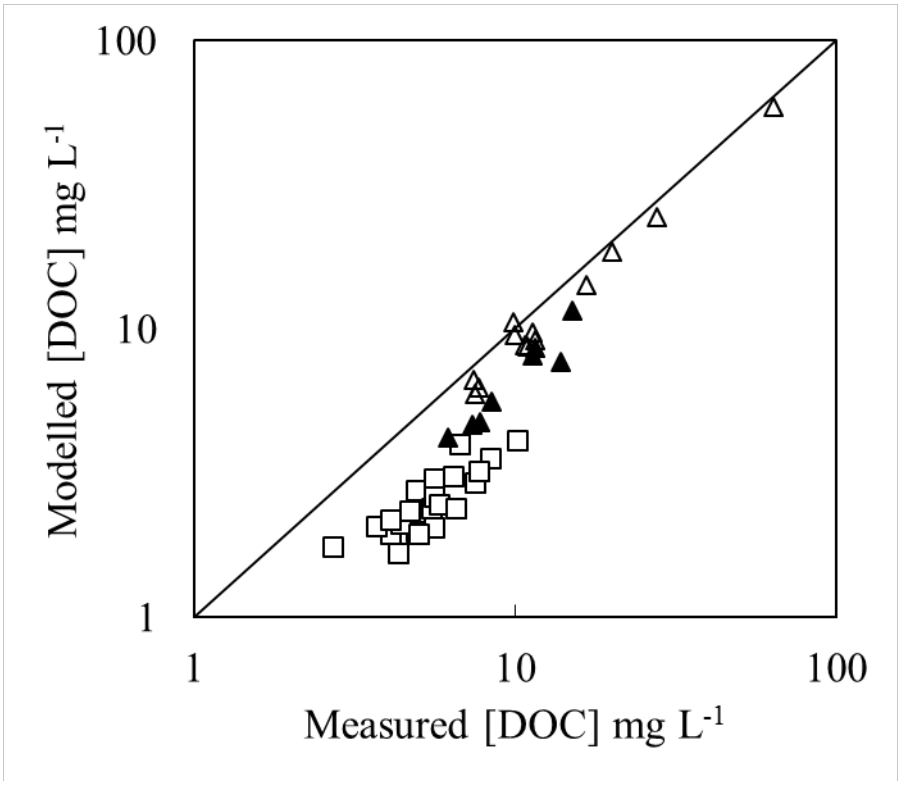

Figure 4

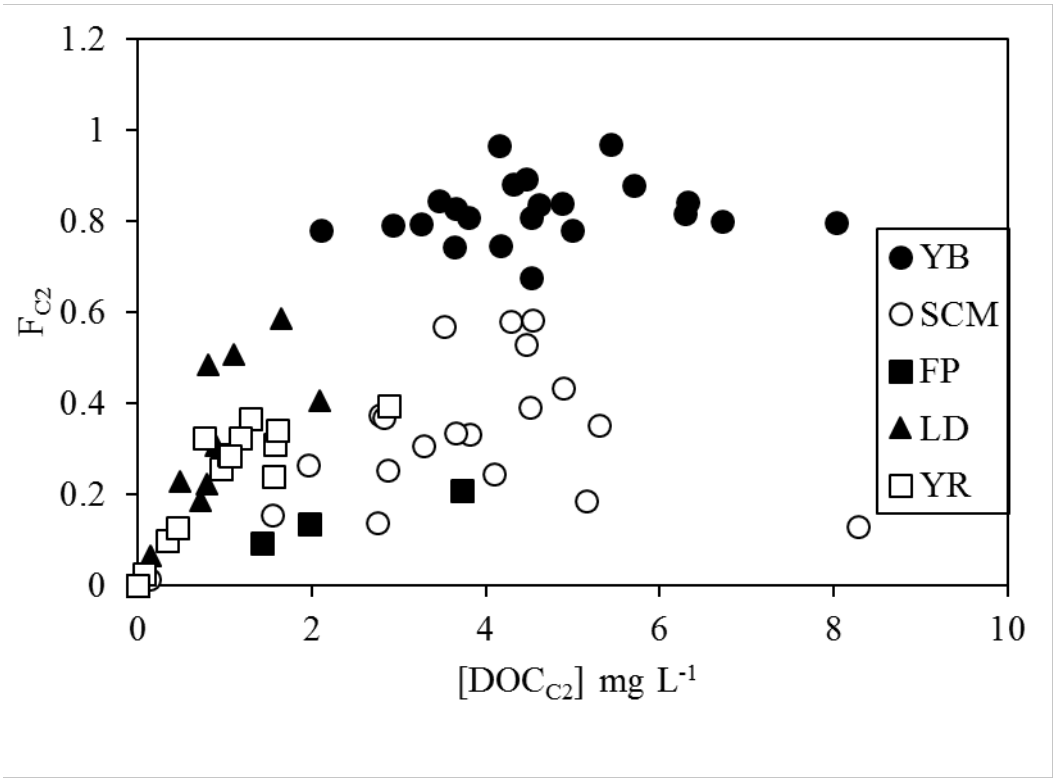

Figure 5

724